

PAPER Nr.: 48



AN INVESTIGATION OF THE COOLING OF ENGINE EXHAUST GASES THROUGH A  
CIRCULATION CONTROLLED TAIL BOOM AND THRUSTER

BY

ALAN NURICK, PIETER BOUWER  
UNIVERSITY OF THE WITWATERSRAND, JOHANNESBURG  
SOUTH AFRICA

**TWENTIETH EUROPEAN ROTORCRAFT FORUM**  
OCTOBER 4 - 7, 1994 AMSTERDAM

# An Investigation of the Cooling of Engine Exhaust Gases Through a Circulation Controlled Tail Boom and Thruster

Alan Nurick                      Pieter Bouwer  
University of the Witwatersrand, Johannesburg

An experimental investigation was carried out to characterise the performance of a helicopter anti-torque system comprised of a thruster, simulated circulation controlled tail boom and a nozzle for ducting engine exhaust gases into the tail boom. Air to the circulation controlled tail boom is conveyed between an inner cylinder and the tail boom wall ensuring that cold air is in contact with the tail boom. Tests were carried out using both hot and cold air to simulate the engine exhaust gases. The performance of both the thruster and nozzle are characterised in terms of dimensionless parameters which are independent of the density of the gases. It was found that power extracted from the engine exhaust gases can contribute significantly to that required to drive the thruster. The temperature of the gases exhausting from the thruster may be predicted by means of a thermal balance and is significantly lower than that of the engine exhaust gases.

## NOTATION

A	=	cross-sectional area of the thruster outlet
C <sub>p</sub>	=	specific heat at constant pressure
f	=	$(P_a - P_f) / (\rho_f V_f^2 - \rho_a V_a^2)$
G	=	mass flow rate
g	=	$(P_e - P_f) / (\rho_f V_f^2 - \rho_e V_e^2)$
K <sub>G</sub>	=	$G_{thr} / (A \rho T)_{thr}^{1/2}$ = flow rate coefficient
K <sub>P</sub>	=	$P (A \rho)_{thr}^{1/2} / T^{3/2}$ = power coefficient
K <sub>T</sub>	=	$T / (A P_c)_{thr}$ = thrust coefficient
P	=	power, static pressure
P <sub>in</sub>	=	$G_a (C_{pa} T_a + V_a^2 / 2) + G_e (C_{pe} T_e + V_e^2 / 2)$
P <sub>out</sub>	=	$G_f (C_{pf} T_f + V_f^2 / 2)$
P <sub>t</sub>	=	total pressure referenced to atmospheric pressure
T	=	temperature, thruster thrust
V	=	velocity
ρ	=	air density

## Subscripts

a = ambient air from the fan flowing to the thruster  
e = engine gases at the nozzle  
f = final mixture of gases at the inlet to the thruster  
thr = thruster  
cctb = circulation controlled tail boom

## 1 INTRODUCTION

A helicopter anti-torque system comprised of a circulation controlled tail boom (CCTB) and a thruster (CCTB@T) was proposed by Velazquez [1] at Lockheed Aircraft Corporation [2] in 1972. CCTB@Ts have been incorporated by McDonnell Douglas Helicopter Company in their MD520N and MDX helicopters [3,4].

The temperature of the exhaust gases of helicopter engines is of the order of 500°C offering significant infra-red signatures to heat seeking missiles. Since the CCTB@T uses ambient air the question was raised by Viljoen [5] whether this air could be used to cool the engine exhaust gases before they are discharged into the atmosphere. An arrangement based on this concept is comprised of the CCTB@T with the engine gases being ducted into the tail boom. It is referred to as a Combined Infra-Red and Tail Rotor Elimination (CIRSTEL) system. A diagrammatic arrangement of a helicopter fitted with a CIRSTEL system is presented in figure 1.

In CIRSTEL the hot engine gases are exhausted through a mixing nozzle into a pipe in the tail boom where they mixed with ambient air supplied by a fan located in the transition piece between the

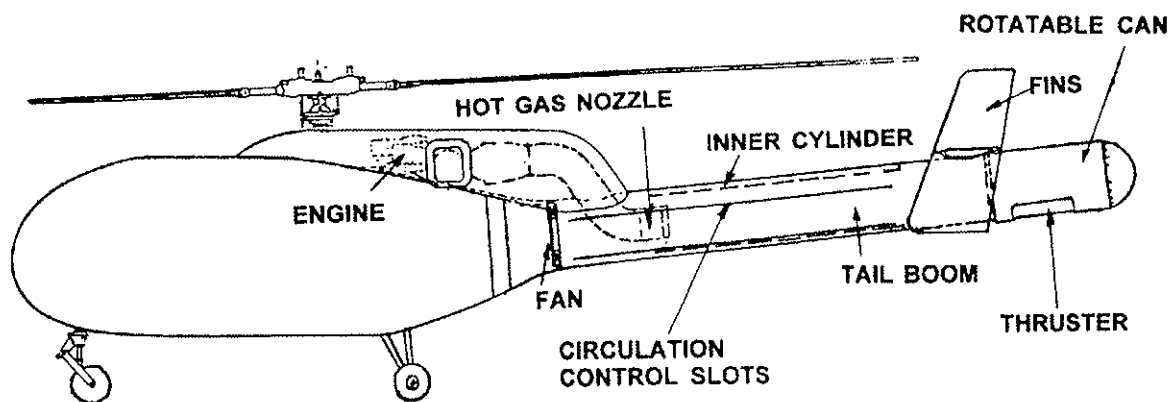


Figure 1 General Arrangement of a Helicopter Fitted with a CIRSTEL System

main body and the tailboom. The gas leaving the mixing pipe is exhausted into the atmosphere through a thruster fitted to the end of the tailboom. The thruster turns the air through approximately 90° to produce a component of the torque required to balance that applied to the main rotor. The tail boom is fitted with an inner cylinder which provides a separate channel for the air supplied to the circulation control slots to prevent it from mixing with the hot gases thereby ensuring that the external surface of the tail boom remains comparatively cool.

An experimental programme was initiated to characterise the performance of such a system with particular emphasis on the mixing nozzle and thruster.

## 2 EXPERIMENTAL EQUIPMENT

Tests were carried out on two rigs viz one in which hot gases at temperatures typical of engine exhaust gases were fed through the mixer nozzle and one in which all air streams were at approximately ambient temperature.

### 2.1 Models

#### Hot Gas Tests

A diagrammatic arrangement of the hot gas test rig is given in figure 2. The engine gas flow was simulated using air from the Hot Gas Test Facility (HGTF) of the Council for Scientific and Industrial Research. Due to the limited space available adjacent to the HGTF it was necessary to bend the duct between the tail boom and cold air fans.

The tail boom consists of a 300mm diameter stainless steel tube with a wall thickness of 0.9mm with two 2mm slots each with a

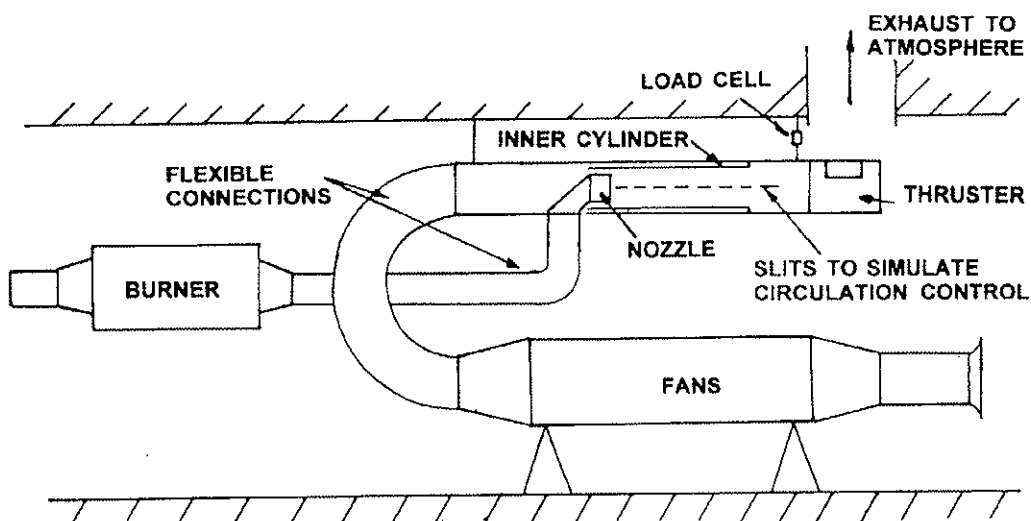


Figure 2 General Arrangement of the Hot Gas Test Rig

length of 1.2m to simulate the flow to the circulation control slots. Fitted inside this tube is a 1.1m long 260mm diameter stainless steel tube which prevents the ambient air flowing to the circulation control slots from mixing with the hot gases. The mixing nozzle (with an average diameter of 250mm and outlet area of 0,0249m<sup>2</sup>) fits into the mixing pipe. A 150mm diameter stainless steel tube (passing through the 300mm diameter pipe) connects the mixing nozzle to the air supply. The HGTF can supply air at temperatures of up to 450°C at 3.5kg/s.

The thruster is bolted on to the end of the 300mm diameter pipe. It has an outlet of 0.387m x 0.2m and is fitted with vanes to facilitate turning the air into the atmosphere.

An advantage of using slits on either side of the tail boom to simulate the air flow to the circulation control slots is that no thrust is developed by this flow which could complicate the measurement of the thruster thrust.

The tail boom is supported at its aft end by means of a load cell to measure the thrust. At the end where the ambient air is ducted into the model it is supported by means of a thin stainless steel plate. The 150mm diameter pipe which connects the mixing nozzle to the burner is fitted with a bellows section to minimize the effects of any movement of the 150mm pipe on the thrust reading.

### Cold Gas Tests

A diagrammatic arrangement of the cold gas test rig is given in figure 3. In this rig the same components used for the hot tests were rearranged to give a straight through flow and the forward end of the tail boom was supported on pivots rather than by a plate. The HGTF was replaced by a fan.

### 2.2 Fans

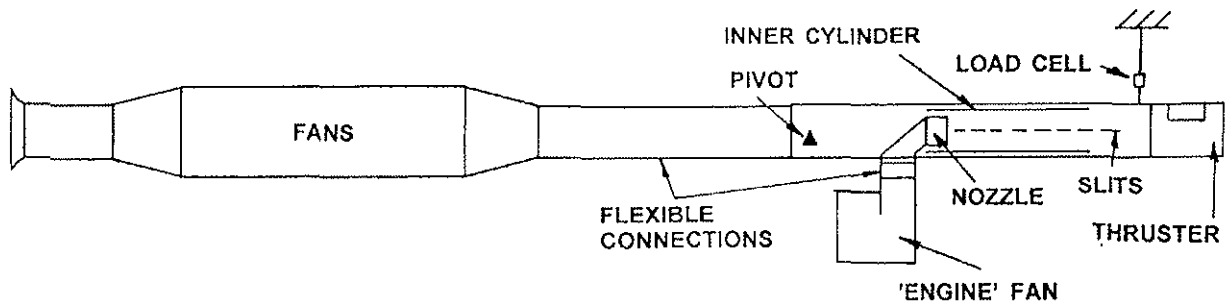


Figure 3 General Arrangement of the Cold Test Rig

A set of four axial fans, connected in series, was used to provide

ambient air to the model. Each fan could be switched on individually allowing 2, 3 or 4 fans to be selected for a test. For both rigs air was ducted into the tailboom by means of a metal reinforced fabric concertina pipe as shown in figures 2 and 3.

### 2.3 Instrumentation

Three Anubars were used to measure the ambient air flow, engine exhaust flow and air flow through the thruster. Pressures were measured using a combination of transducers and a scanivalve. All transducer signals were fed to an MUX-Card connected to a personal computer. The software used to read the MUX-Card was specifically developed for the test rig at the HGTF. Data read during a test are automatically saved on disc in ASCII format from where they may be processed at a later stage.

The standard deviations of the instrumentation used on the test rigs is presented in table 1.

Table 1 Instrumentation Standard Deviations

TRANNSDUCER	RANGE	STANDARD DEVIATION
Cold air flow rate	5000 Pa	4.33 Pa
Engine flow rate	1200 Pa	3.89 Pa
Thruster flow rate	5000 Pa	3.40 Pa
Scanivalve	5000 Pa	4.31 Pa
Thruster load cell	500 N	6.53 N

## 3 TEST PROCEDURE

Tests were carried out with varying flow rates of air from the cold air fans and simulated engine flow. For the hot gas tests the burner was started first and allowed to stabilise at a temperature of 450°C with a flow rate to the burner of 0,3 kg/s. Then the selected number of cold air fans (2,3 or 4) was switched on and the flow rate to the burner adjusted to between 0,3 kg/s and 1,1 kg/s. Each data point was averaged from ten readings.

## 4 RESULTS AND DISCUSSION

### 4.1 Mass Flows

The mass flows relevant to the performance of CIRSTEL which could conveniently be used to characterise its performance are:

- i The flow from the burner (primary flow) ( $G_e$ )
- ii The ambient air from the fans (secondary flow) ( $G_{cctb}+G_a$ )

- iii The air flow to the circulation control slots ( $G_{cctb}$ ), and
- iv The flow to the thruster ( $G_f = G_b + G_a$ )

It has been shown [6] that the flow to the thruster is given by:

$$K_G = \frac{G_{thr}}{(A \rho T)_{thr}^{1/2}} \quad (1)$$

with  $K_G = 0.8869$  and a standard deviation of 0,0303 for the tests given in reference 6. In the case of the hot tests the Annubar used to measure the mass flow to the thruster was found to be inaccurate and for those tests the total mass flow to the thruster ( $G_f$ ) was determined using equation (1).

For the hot tests the flow rate to the circulation control slots was determined as the difference between the sum of the flows to the burner and fans and that calculated for the thruster.

Alternatively the flow rate to the circulation control slots may be calculated from:

$$G_{cctb} = \frac{t}{D} D 0,8 (2 \rho P_s)^{1/2} \quad (2)$$

where the total slot width to boom diameter  $t/D$  was 0.014 as was used in reference 7. The factor 0,8 is an empirical constant [8].

The flow rates to the CCTB slots used in the experiments was on average 41.6% of the calculated values. It varied from 0.11 kg/s to 0.37 kg/s. The flow rate to the CCTB was not taken into account in determining the performance of the thruster.

#### 4.1 Thruster Thrust

It has been shown [6] that the thrust of the thruster is given by:

$$T = K_T (A P_t)_{thr} \quad (3)$$

Data obtained from both the hot and cold tests required to determine  $K_T$  are presented in figure 4.

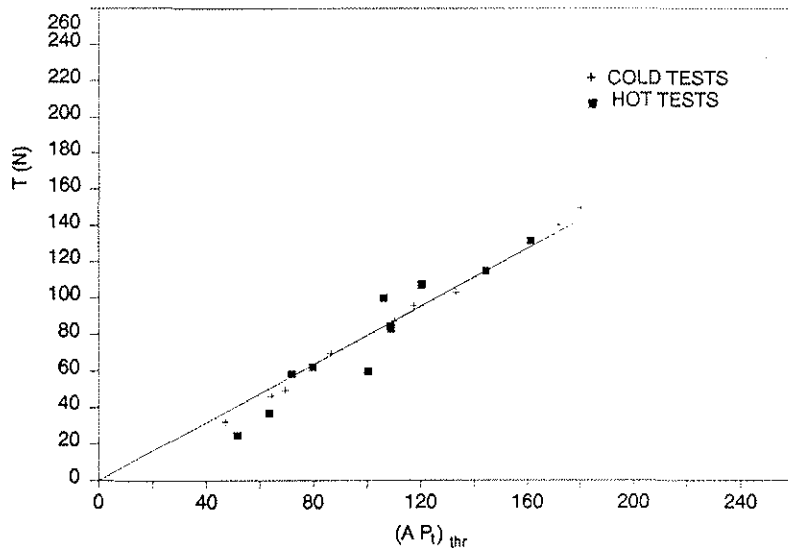


Figure 4 Variation of Thruster thrust with  $(A P_t)_{thr}$

It was found for these tests that  $K_T=0.794$  with a correlation coefficient of 0.977. The value of  $K_T$  may be expected to be a function of the geometry of the thruster but it appears from the data obtained for these tests that  $K_T$  is independent of the density of the air for a given geometry and is not affected by the temperature of the air.

#### 4.3 Power

It has been shown [6] that the power of the air supplied to the thruster is given by:

$$P = K_p \frac{T^{3/2}}{(A \rho)_{thr}^{1/2}} \quad (4)$$

Data obtained from both the hot and cold tests required to determine  $K_p$  are presented in figure 5.

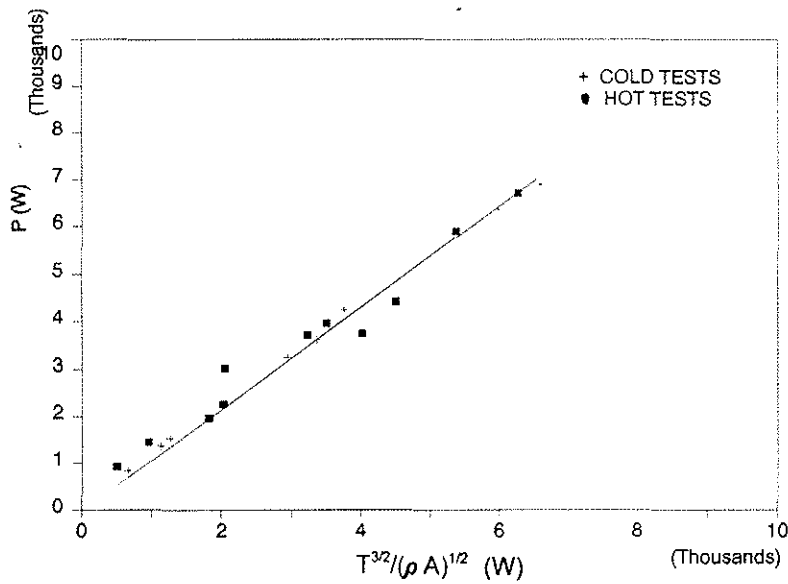


Figure 5 Variation of Thruster Power with  $T^{3/2}/(\rho A)_{thr}^{1/2}$

It was found for these tests that  $K_p=1.0750$  with a correlation coefficient of 0.989. The value of  $K_p$  may be expected to be a function of the geometry of the thruster but it appears from the data obtained for these tests that  $K_p$  is independent of the density of the air for a given geometry and is not affected by the temperature of the air.

The total power supplied to the thruster will be at least the sum of the powers supplied by the fan and that contained in the exhaust gases from the engine. Due to the difference in velocities between the air from the fan and the engine gases flowing out of the nozzle and the consequent shear stresses between the two air streams prior to their being mixed it is not possible to determine in a simple manner how the energy to the thruster is constituted. To obtain an indication of the power required from the fan at various mass flow ratios an equivalent power factor  $K_{pfan}$  was calculated using:

$$K_{pfan} = \frac{P_{fan} (A \rho)_{thr}^{1/2}}{T^{3/2}} \quad (5)$$

In equation (5) the thrust is the total thrust developed by the thruster while the power is that attributed to the fan only. Since it may be expected that interaction of the engine and exhaust gases

will depend on the relative velocity between the two airstreams the variation of  $K_{p_{fan}}$  with velocity ratio  $V_e/V_a$  for both the hot and cold tests is examined in figure 6.

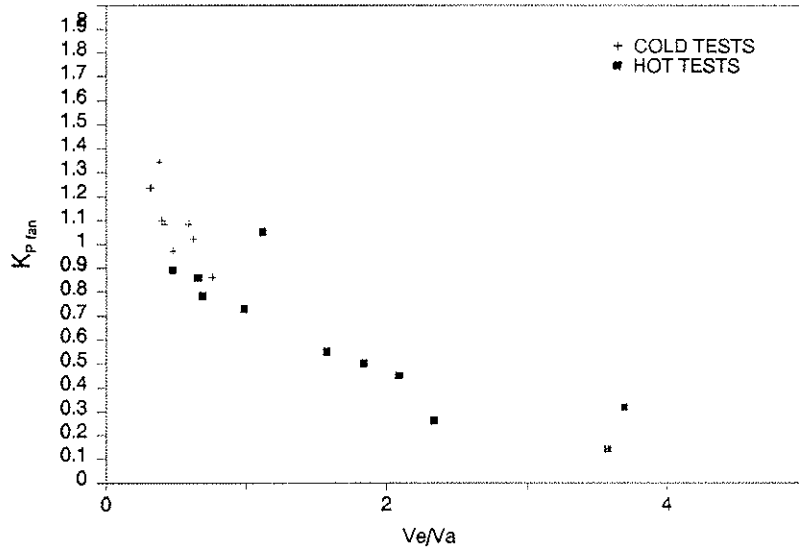


Figure 6 Variation of  $K_{p_{fan}}$  with Velocity Ratio  $V_e/V_a$

As may be seen from figure 6  $K_{p_{fan}}$  is strongly dependent on the ratio of the velocity of the engine gases exiting from the nozzle to that of the cold air flowing past the nozzle and it appears that  $K_{p_{fan}}$  is independent of the temperature (or density) of the engine exhaust gases. The data in figure 6 indicate that the power in the engine exhaust gases can contribute significantly to that required for the thruster. The dependence of  $K_{p_{fan}}$  on  $V_e/V_a$  indicates that the power contributed by the engine exhaust gases to that applied to the thruster could be controlled by varying the area ratio of the nozzle outlet to that of the inner cylinder in the tail boom.

It may be expected that the balance of the power required for the thruster would be supplied by the exhaust gases and hence it would be expected that:

$$K_{P_e} = \frac{(P - P_{fan}) (A \rho)_{thr}^{1/2}}{T^{3/2}} = \frac{P_e (A \rho)_{thr}^{1/2}}{T^{3/2}} \quad (6)$$

#### 4.4 Static Pressure

##### Static Pressure Drop of the Cold Air

The static pressure drop of the air supplied by the fan from a point upstream of the nozzle to the inlet of the thruster should be quantified to demonstrate that the pressure of the air in the circulation controlled slots will be high enough to ensure that the torque developed by the CCTB is adequate.

The static pressure drop from the cold air fan exhaust to the thruster inlet will depend on a number of factors including the change in total energy of the air per unit mass due to mixing of the engine exhaust and fan air, turbulent shear stresses and losses due to factors such as flow expansions. The difficulty of predicting the performance of nozzles is discussed in reference 9.

A momentum balance across the tail boom duct over the area  $A_B - A_e$  of flow of the fan air past the nozzle, ignoring shear stresses and flow across the control volume gives:

$$P_a - P_f = \rho_f V_f^2 - \rho_a V_a^2 \quad (7)$$

Dividing equation (7) by the RHS and assuming that the resulting dimensionless relationship will be a function of parameters including the mass flow ratio  $G_e/G_a$  rather than having a value of unity gives:

$$\frac{P_a - P_f}{\rho_f V_f^2 - \rho_a V_a^2} = f\left(\frac{G_e}{G_a}\right) \quad (8)$$

where  $f$  is a function of the mass flow ratio. To determine whether such a function for the geometry of the CIRSTEL tail boom tested exists  $f$  was plotted against the mass flow ratio as shown in figure 7.

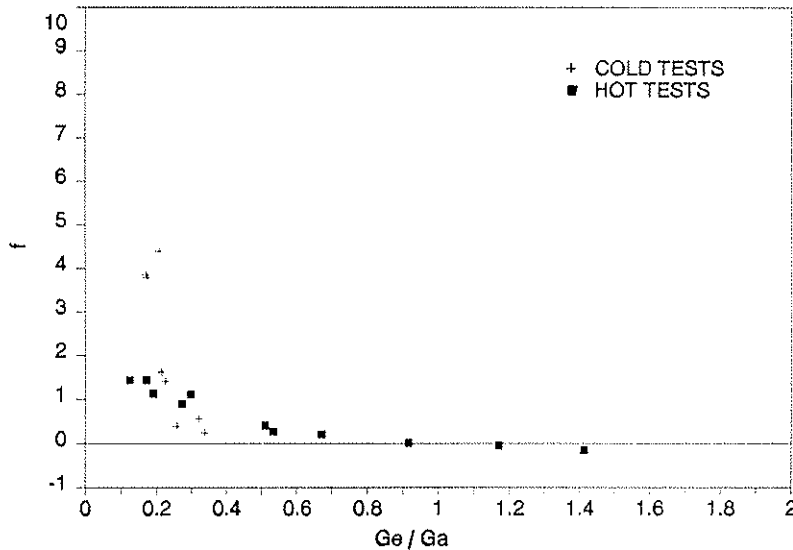


Figure 7 Variation of f with Mass Flow Ratio

From the data presented in figure 7 it appears for the tests carried out that to good approximation f is a function of the mass flow ratio. At low mass flow ratios the static pressure drop across the nozzle is high demonstrated by values of f of the order of 4. As the mass flow ratio is increased so the static pressure difference between the fan exit and the thruster inlet reduces indicating energy is transferred to the cold air from the hot gases resulting in increased static pressure. At mass flow ratios greater than approximately 1 the static pressure of the cold air between the two stations of interest increases.

It is likely that CIRSTEL will operate with the mass flow ratio greater than 0.25 and consequently f will be less than unity and the static pressure drop of the cold air will not be significant.

**Static Pressure Drop of the Engine Exhaust Gases**

The static pressure of the air at the outlet of the engine will be given by the static pressure at the nozzle plus the static pressure drop in the duct from the engine outlet to the nozzle. As the back pressure can affect the performance of the engine it is necessary to quantify the static pressure at the nozzle to ensure that it is not too high at any stage of the flight envelope.

Using arguments similar to those used for the cold air static pressure the static pressure difference between the mixing nozzle and inlet to the thruster gives:

$$\frac{P_e - P_f}{\rho_f V_f^2 - \rho_e V_e^2} = g \left( \frac{G_e}{G_a} \right) \quad (9)$$

where as before it is assumed that  $g$  is a function of the mass flow ratio. To determine whether such a function exists for the geometry of the CIRSTEL tail boom tested the left hand side of equation (9) was plotted against the mass flow ratio as shown in figure 8.

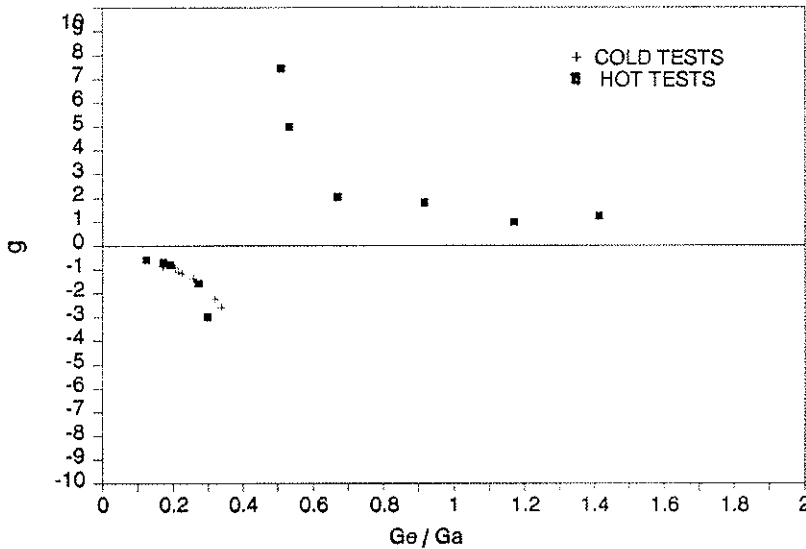


Figure 8 Variation of  $g$  with Mass Flow Ratio  $G_e/G_a$

It appears from the data presented in figure 8 that for the case tested  $g$  is in fact a function of the mass flow ratio for the hot gas tests over the range of mass flow ratios tested and at low mass flow ratios for the cold tests.

At low mass flow ratios the denominator of equation (9) will be negative i.e.  $\rho_f V_f^2 - \rho_e V_e^2 < 0$  and  $P_e > P_f$  with the static pressure in the nozzle being strongly affected by that of the cold air flow. As the mass flow ratio increases  $\rho_f V_f^2 - \rho_e V_e^2$  will pass through zero resulting in the large values of  $g$ . Correlation of the available velocity ratios with mass flow ratios indicated that for the test configuration tested  $V_e = V_a$  at  $G_e/G_a = 0.373$ . At larger values of the mass flow ratio  $\rho_f V_f^2 - \rho_e V_e^2 > 0$  with  $P_e < P_f$  this being consistent with the conservation of energy of the engine gases.

At large mass flow ratios the flow of cold air becomes less significant with respect to the pressure distribution in the tail

boom with the flow tending to that of a single flow stream comprised essentially of the flow from the engine exhaust with a constant total energy per unit mass. In this situation the loss of energy of the exhaust gas from the exit of the nozzle to the inlet of the thruster will be low and  $g$  will tend to a value of unity.

It appears from the data that at low mass flow ratios it may be necessary to ensure that the back pressure on the engine does not become a problem.

#### 4.5 Temperature

Infra red signatures can be generated by any hot component of the helicopter. In the case of the CIRSTEL system two major sources of an infra-red signature are the hot gases exhausting out of the thruster and the temperature of the wall of the tail boom.

#### Thruster Jet

For the case where energy losses from the system are negligible an energy balance gives:

$$G_f (C_{P_f} T_f + \frac{V_f^2}{2}) = G_a (C_{P_a} T_a + \frac{V_a^2}{2}) + G_e (C_{P_e} T_e + \frac{V_e^2}{2}) \quad (10)$$

The specific heat of the gases is given by [10]:

$$C_p = 1,0036 + 0,0702 \cdot 10^{-3} T + 0,1715 \cdot 10^{-6} T^2 - 0,0702 \cdot 10^{-9} T^3 \quad (11)$$

To obtain an indication of the overall loss in energy occurring in the tail boom the energy entering the thruster defined by the LHS of equation (10) was compared with that entering the system i.e. the RHS of equation (11). The data are presented in figure 9.

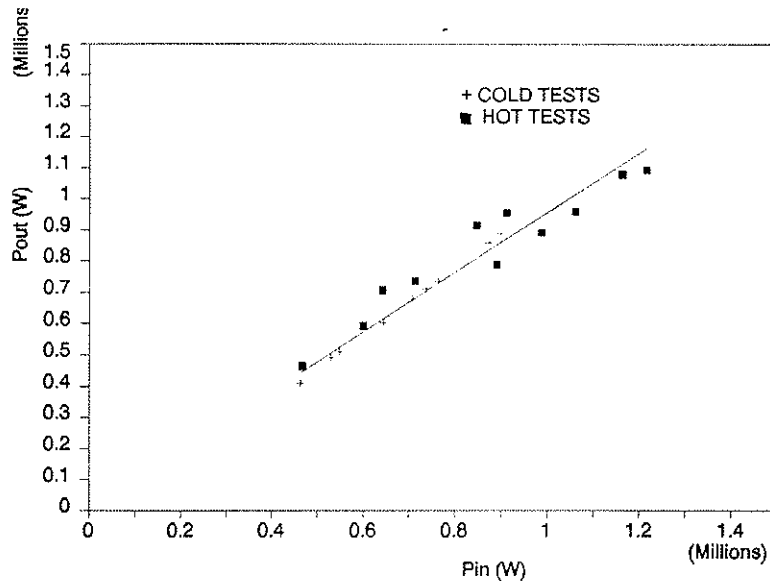


Figure 9 Variation of  $P_{out}$  With  $P_{in}$

It was found from the data that  $P_{out}=0.9562 P_{in}$  with a correlation coefficient of 0.9675. Thus it appears a loss of power of 3.25% of the input power is lost in the system.

For the tests carried out the kinetic energy of the gases was less than 0.5% of the total internal energy of the gas. Thus equation (10, on averaging  $C_{pf}$ , may be approximated to give:

$$T_f = \frac{C_{pe} T_e \left(\frac{G_e}{G_a}\right) + C_{pa} T_a}{C_{pe} \left(\frac{G_e}{G_a}\right) + C_{pa}} \quad (12)$$

It is clear from equation (12) that apart from the small variation of  $C_p$  with temperature and consequently with the mass flow ratio the temperature of the thruster jet is a function of the mass flow ratio and of the temperatures of the nozzle and ambient air.

In figure 10 the variation of measured temperature with mass flow ratio is compared with the value of  $T_f$  obtained using equation (12).

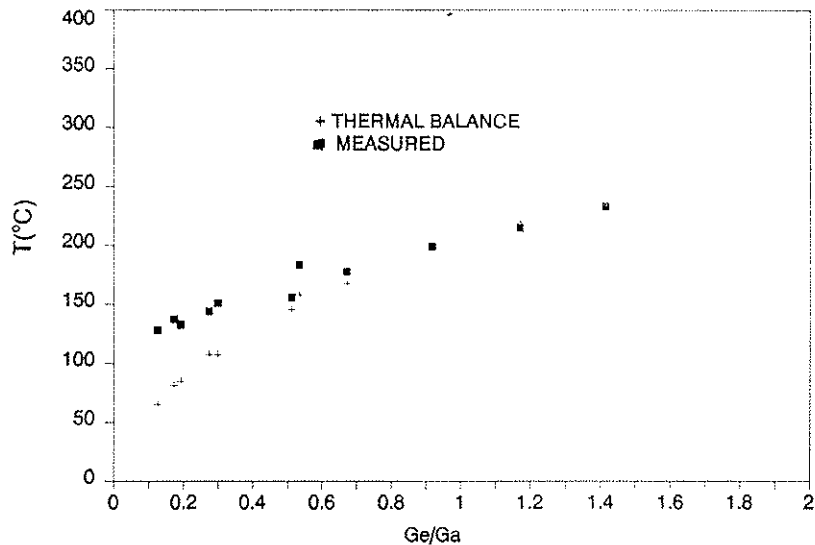


Figure 10 Variation of Exhaust Gas Temperature with Mass Flow Ratio

As may be seen in figure 10 good correlation was obtained between the measured and expected temperatures of the gases in the thruster at mass flow ratios greater than 0.45. At lower mass ratios the measured temperature of the exhaust gases was higher than that calculated from the mass flows and temperatures of the engine exhaust and cold air flows. The reason for the difference has not been established but may be attributed to errors in the mass flows.

The temperature of the nozzle exhaust gases was approximately 450°C.

#### Tail Boom Skin

The temperature of all solid surfaces should be kept as low as possible as hot surfaces can offer significant IR signatures. In figure 11 the temperature difference between the surface of the tail boom and the atmospheric temperature is presented as a function of the mass flow ratio. While it is accepted that this temperature difference will be a function of more parameters than the mass flow ratio the data are presented to give an indication of possible temperature differences and to demonstrate that the temperature differences are not large for the system tested.

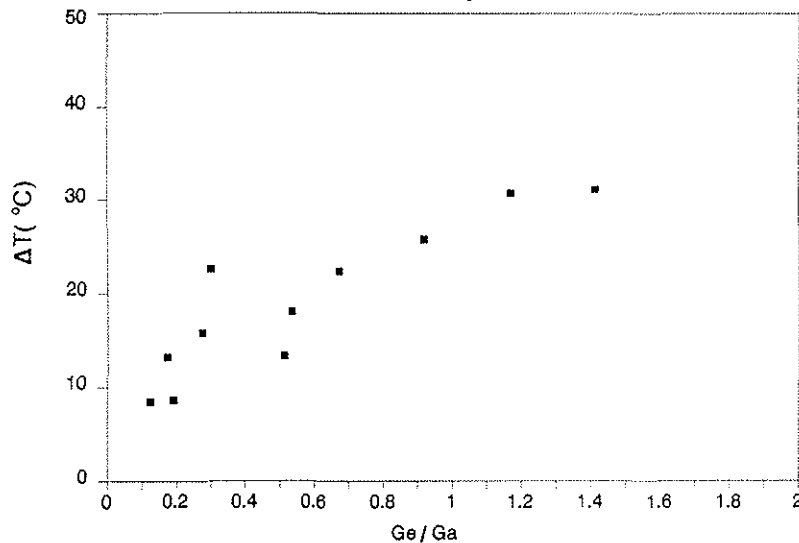


Figure 11 Variation of Tail Boom Wall Temperature with Mass Flow Ratio

As shown in figure 11 and as may be expected the temperature difference increases with lower ambient air flow rates. It should be noted, as was mentioned above, the flow to the circulation control slots was less than the scaled calculated values and it is likely that the temperature of the surface of the tail boom will be lower than that measured and presented in figure 11.

## 5 CONCLUSIONS

- i the behaviour of the thruster can be expressed in terms of  $K_T$  and  $K_p$  and these values for a given geometry are not materially affected by the density of the air
- ii the power of the engine exhaust gases contribute to that required to drive the thruster thereby reducing the power of the cold air fan
- iii it is possible to describe the reduction in fan power in terms of  $K_{p_{fan}}$  with the variation of  $K_{p_{fan}}$  being a function of the mass flow ratio and it appears that  $K_{p_{fan}}$  is a function of the velocity ratio  $V_e/V_a$
- iv since  $K_{p_{fan}}$  is a function of  $V_e/V_a$  it may be expected that the power extracted from the engine exhaust gases could be controlled by selecting the area ratio of the nozzle and inner cylinder
- v the normalised change in static pressure of the fan air between a point upstream of the nozzle and the inlet to the thruster may be described in terms of the mass flow ratio

vi the normalised change in static pressure of the engine exhaust gases between a point in the nozzle and the inlet to the thruster may be described in terms of the mass flow ratio

vii the temperature of the exhaust gases of a typical CIRSTEL system is significantly reduced

viii the temperature of the gases exhausting from the thruster may be readily predicted from considerations of the mass flows with the gas temperature being slightly higher at low mass flow ratios than those predicted

ix the increase in temperature of the wall of the tail boom, without an external airflow, above the ambient temperature is related to the mass flow ratio if the inlet temperatures are kept constant. It appears that the increase in temperature of the walls is of the order of 15/20°C for the geometry tested. If the correct mass flows to the slots is used this temperature rise could be less than that measured.

The results presented provide a basis for the design of a CIRSTEL system. These need to be combined with those of a CCTB and the resulting system balanced to provide the main rotor anti-torque required.

## 8 REFERENCES

- 1) R W Prouty, A Tale of No Tail: MHDC's NOTAR Rotor and Wing, February 1993
- 2) Advanced Anti-Torque Concepts, Lockheed Aircraft Corporation
- 3) A H Logan, Design and Flight Test of the No Tail Rotor (NOTAR) Aircraft, 38th Annual National Forum of the American Helicopter Society, Anaheim, California, May 1982
- 4) E Sampatacos, MD Explorer Development and Test 19th European Rotorcraft Forum, Cernobbio, Italy, 14-16 September 1993
- 5) K Viljoen and A Nurick Private Discussion, November 1992
- 6) A Nurick, An Experimental Investigation of the Static Performance of a Helicopter Thruster, School of Mechanical Engineering Research Report No. 95, University of the Witwatersrand, March 1994
- 7) J R van Horn, NOTAR (No Tail Rotor) Hover testing Using a Scale Model in Water, McDonnell Douglas Helicopter Company, Mesa, Arizona
- 8) A Nurick and C Groesbeek, Experimental and Computational Investigation of a Circulation Controlled Tail Boom, Paper BO5, Eighteenth European Rotorcraft Forum, Avignon, France, 15-

18 September 1992

- 9) F Toulmay, Internal Aerodynamics of Infrared Suppressors for Helicopter Engines, 40th Annual national Forum of the American Helicopter Society, Arlington Virginia, May 16-18, 1984
- 10) K A Kobe, Thermochemistry for the Petrochemical Industry, Petrol, Refiner., January 1949 - November 1954

erf20pap